AAPS PharmSciTech 2004; 5 (3) Article 47 (http://www.aapspharmscitech.org).

Measurement of Fluid Viscosity at Microliter Volumes Using Quartz Impedance Analysis

Submitted: April 21, 2004; Accepted: August 5, 2004.

Atul Saluja,[1] and Devendra S. Kalonia[1]

[1]Department of Pharmaceutical Sciences, School of Pharmacy, University of Connecticut, Storrs, CT 06269

ABSTRACT

The purpose of this work was to measure viscosity of fluids at low microliter volumes by means of quartz crystal impedance analysis. To achieve this, a novel setup was designed that allowed for measurement of viscosity at volumes of 8 to 10 μL. The technique was based on the principle of electromechanical coupling of piezoelectric quartz crystals. The arrangement was simple with measurement times ranging from 2 to 3 minutes. The crystal setup assembly did not impose any unwanted initial stress on the unloaded quartz crystal. Quartz crystals of 5- and 10-MHz fundamental frequency were calibrated with glycerol-water mixtures of known density and viscosity prior to viscosity measurements. True frequency shifts, for the purpose of this work, were determined followed by viscosity measurement of aqueous solutions of sucrose, urea, PEG-400, glucose, and ethylene glycol at 25°C ± 0.5°C. The measured viscosities were found to be reproducible and consistent with the values reported in the literature. Minor inconsistencies in the measured resistance and frequency shifts did not affect the results significantly, and were found to be experimental in origin rather than due to electrode surface roughness. Besides, as expected for a viscoelastic fluid, PEG 8000 solutions, the calculated viscosities were found to be less than the reported values due to frequency dependence of storage and loss modulus components of complex viscosity. From the results, it can be concluded that the present setup can provide accurate assessment of viscosity of Newtonian fluids and also shows potential for analyzing non-Newtonian fluids at low microliter volumes.

KEYWORDS: viscosity, quartz crystal, impedance analysis, Newtonian fluids, viscoelastic fluids.

INTRODUCTION

Various methods and techniques exist for the measurement of fluid viscosity ranging from viscometers that are based on the principle of measuring the time required for a fluid to flow through thin capillaries to fluid shearing viscometers that shear the fluid between rotating cup and bob or cone and plate type assemblies.[1,2] The volume of the liquid sample required by these viscometers can vary from a few hundred microliters to milliliters. A specialized capillary flow viscometer marketed by the Cannon Instrument Co (State College, PA), the Cannon Manning Semi-Micro Viscometer, can use a minimum volume of 0.5 mL of liquid sample just like the cone and plate type viscometer marketed by Brookfield Engineering Laboratories (Middleboro, MA). The most commonly used rotating cup and bob type viscometer, the Brookfield Viscometer, can go to a minimum of 2 mL sample volume with a specialized small sample adapter accessory, whereas the minimum sample required for an Anton Paar (Ashland, VA) Automated Falling Sphere Microviscometer is 150 μL. However, certain pharmaceuticals and biological fluids are either expensive or are available in extremely limited quantities. This is especially true for solutions of novel molecules that are in early stages of pharmaceutical development and only a few milligrams or less of these compounds are available. The rheological analysis on these compounds must be performed using microliter volumes.

Ultrasonic shear rheometry is a promising technique for rheological analysis of liquids and films and nondestructive testing of materials.[3] The pioneering work in this field was done by Mason and coworkers[4,5] who studied viscosity and high-frequency elasticity of several polyisobutylene fluids at ultrasonic frequencies by employing quartz crystal vibrating in the torsional and shear modes. Since then the technique has evolved as a nonconventional means of assessing rheological characteristics of various fluids. Various workers have employed this technique for assessing fluid properties at milliliter volumes[6-9] as well as for studying viscoelastic properties of network forming gels[3,10] and thin polymeric films.[11-13]

Ash et al[14] have employed quartz crystals oscillating at 10 MHz for viscosity measurement of certain industrial oils at volumes of 0.5 μL. However, measurements at such low volumes are practically not feasible for aqueous solutions as evaporation effects on fluid density and viscosity will predominate within the time scale of making any such measurement. Kudryashov et al[3] have monitored gelation of acidified milk at volumes of 1 mL by placing the quartz crystal between 2 viton o-rings followed by fixing a glass tube onto the crystal that served as the sample holder. This design is not much different from cells that are available for conducting surface mass

Corresponding Author: Devendra S. Kalonia, U-2092, Department of Pharmaceutical Sciences, School of Pharmacy, University of Connecticut, Storrs, CT 06269. Tel: (860) 486-3655. Fax: (860) 486-4998. Email: kalonia@uconn.edu.

change experiments based on quartz crystal microbalance technique. Although simple to design, such a setup places an initial stress on the quartz crystal leading to an increase in the crystal damping (losses) even before any liquid sample is placed on the crystal. These initial losses indirectly affect the stability and reproducibility of the oscillation through their effect on the quality factor (Q) of the quartz crystal.[15] For such a setup, the time required for an unloaded crystal, ie, crystal that is still not loaded with the test liquid, to stabilize is greater, which leads to longer measurement times. In addition, there is a slow drift in the losses for an unloaded crystal itself with time, which is difficult to control and account for. Alternative arrangements are available that employ adjustable crystal holding assemblies in order to regulate the initial stress on the crystal, but then leakage of the test liquid beyond the electrode region of the crystal can lead to fringe effects and inconsistencies in the area covered by the liquid.

In this paper, we present a novel setup based on the principle of ultrasonic shear rheometry for measuring viscosity of pharmaceutically relevant aqueous solutions at low volumes of 8 to 10 µL and discuss various factors that can have a bearing on the consistency of the results. The arrangement is simple and as the crystal itself is not compressed between any o-rings or holding assemblies, initial stabilization of an unloaded crystal is fast and there are no unwanted stresses or losses imposed on the crystal. This technique provides a control over the area being covered by the test liquid, experimental ease in terms of short testing times of around 2 to 3 minutes, and ease of washing and handling of crystals between successive experiments.

Impedance Analysis of Quartz Crystals

Piezoelectric Viscosity Sensor

The piezoelectric quartz crystal forms the heart of the viscometer discussed here. When pressure or deformation is applied to a properly cut quartz crystal, a separation of charges occurs that leads to a build up of a potential difference across the 2 ends of the crystal with the magnitude of the developed potential difference being proportional to the applied stress. The *converse piezoelectric* effect, on which the discussed viscometer is based, involves a deformation of the quartz crystal resulting from the application of a potential difference across the crystal faces. As and when the applied potential is reversed, the crystal deforms in the opposite direction resulting in mechanical vibrations. AT cut crystals vibrating in the thickness shear mode (TSM), with displacement parallel to the surface, are used for such applications. AT refers to a specific orientation at which the crystal is cut from the quartz bar in order to yield a low temperature coefficient i.e. shift in the crystal frequency with temperature. Shear mode vibrations are excited in the crystal at frequencies for which the thickness of the quartz crystal corresponds to an odd multiple of half of the acoustic wavelength.[16] A quartz crystal microbalance (QCM), discovered by Sauerbrey[17] in 1959, uses this setup to measure mass changes in the nanogram range as mass deposited on the electrode causes a decrease in the resonant frequency of the quartz crystal due to an increased thickness of the electrode.

A QCM can be used as a sensitive density and viscosity detector when operated in liquids as long as there is physical coupling between the quartz electrode and the liquid and molecular slip does not occur[18] (some authors[19] disagree with "interfacial slip" theory and attribute a poor physical coupling to presence of intervening gas phase). In 1985, Kanazawa and Gordon[8] derived the following relationship between the frequency shift and the viscosity-density product:

$$\Delta f = -f_U^{3/2}\sqrt{\frac{\rho_{Liq}\eta_{Liq}}{\pi\mu_q\rho_q}} \qquad (1)$$

where Δf is the frequency shift occurring on mass loading, f_U is the crystal frequency under no load, μ_q is the crystal shear modulus (2.947×10^{11} gm/cm/sec^2), ρ_q is the crystal density (2.651 g/cm^3), and ρ_{Liq} and η_{Liq} represent the liquid density and viscosity, respectively. However, with frequency shift being the only measured variable, it is not possible to distinguish between mass effects and the density-viscosity effects as both bring about a decrease in the crystal resonance frequency. Impedance analysis around crystal resonance frequency can simultaneously monitor resistance (damping) and frequency shifts and is thus able to separate these 2 effects.

Electrical Properties of Quartz and Electromechanical Coupling

The electrical properties of a quartz crystal can be described by means of a Butterworth van-Dyke (BVD) model of lumped electrical parameters also known as the lumped-element model (LEM) (Figure 1). R_1 represents the losses in the crystal, frictional, or thermal; L_1 represents the inertial mass of the crystal; and C_1 is a measure of the energy stored in the crystal during each oscillation. The complex impedance of a quartz crystal can be represented by the following relationship:

$$Z = R + jX \qquad (2)$$

Unlike resistance, inductive and capacitive impedance are frequency dependent and together form the reactive or the imaginary part of the complex crystal impedance (X)

$$X = 2\pi fL_1 - \frac{1}{2\pi fC_1} = \omega L_1 - \frac{1}{\omega C_1} \qquad (3)$$

with ω being the angular frequency in radians/sec. The ratio of the reactive part to the resistive part is defined as the phase

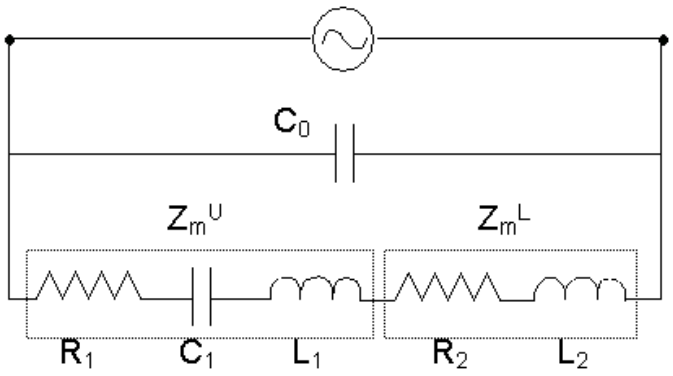

Figure 2. Modified Butterworth van-Dyke model for a loaded quartz crystal showing additional impedance elements imposed due to placement of load on the surface of the quartz crystal electrodes. Z_m^U refers to the electrical impedance of the motional arm under condition of no load and Z_m^L refers to the electrical impedance imposed due to the load.

Figure 1. The Butterworth van-Dyke (BVD) or lumped element model (LEM) for a quartz crystal showing the individual electrical components.

angle (θ). At a particular frequency, the inductive and the capacitive contributions of the motional arm are equal, and the reactive part reduces to zero, thereby minimizing the impedance of the crystal to just the resistive losses. This frequency is defined as the *series resonant frequency* f_s as at this frequency the phase angle is zero and impedance of the motional arm is at a minimum ($Z = R_1$). The voltage and current are in phase at this frequency. Similar to crystal impedance, its inverse, admittance, can also be used to describe the quartz crystal. The series resonant frequency is characterized by a maximum in the frequency-admittance plot.

$$Y = G + jB \tag{4}$$

where, *Y* is admittance, *G* is conductance, and *B* is susceptance. At series resonant frequency just as both phase and reactance reduce to 0, so does susceptance. At these points conductance equals $1/R_1$.

By means of impedance analysis, one can determine quantitatively how shifts in the circuit parameters upon loading relate to the physical properties of the load. As a result of loading the quartz crystal electrode with liquid, the electrical parameters of the crystal are modified and can be represented as a modified Butterworth van-Dyke model (Figure 2). The changes in the crystal capacitance on loading are extremely small and are not considered for liquid loadings.[20]

The principle behind the use of a quartz crystal for measurement of fluid rheology is that of electromechanical coupling between the mechanical properties of the load and electrical properties of the crystal.[21,22] R_2 and L_2 (electrical impedance parameters) obtained after impedance analysis are used to calculate the mechanical impedance of the load (Z_s^L), which is defined as the ratio of the surface stress to particle velocity at the surface with units of gm/sec/cm^2. Just like electrical impedance of the motional arm (Z_m), Z_s is also a complex quantity consisting of a real lossy (viscous) part and an imaginary storage (inertial mass/storage) part. Z_m^L and Z_s^L (impedance under load) are related through a constant (A) comprising of the electromechanical coupling constants, the crystal fundamental resonance frequency and mode, piezoelectrically active area, and unloaded quartz impedance as follows[23]:

(5)

where R_2 is the real component of the motional impedance due to the surface load, $X_2 = \omega L_2$ is the imaginary component of the motional impedance due to the surface load, N is the overtone number, K^2 is the piezoelectric coupling constant = 7.74×10^{-3} (dimensionless), ω_s is the series resonant frequency (radians/sec), C_0 is the static plus stray capacitance (farads), and Z_q is the quartz mechanical impedance = 8.839 $\times 10^5$ gm/sec/cm^2, which equals $(\mu_q \rho_q)^{1/2}$. The constant term for a specific frequency crystal, ie, $\frac{N\pi}{4K^2\omega_s C_o Z_q}$ is grouped together to give the constant A. Thus, R_2 is proportional to the real part of the mechanical impedance ($R_2 \propto \mathrm{Re}\,(Z_s)$) and X_2 is proportional to the imaginary part of mechanical impedance ($X_2 \propto Im\,(Z_s)$) through the constant A.[24]

Calculation of Circuit Parameters and Load Impedance

Under conditions of a load being placed on the crystal, the circuit admittance is represented as

$$Y = j\omega C_0 + 1/Z_m \tag{6}$$

and its magnitude is given by the following relationship[20]:

(7)

$R_m = R_1$, $L_m = L_1$, and $C_m = C_1$ for unloaded crystal and $R_m = R_1 + R_2$, $L_m = L_1 + L_2$, and $C_m = C_1$ for loaded crystal. The modified BVD model (Figure 2, Equation 7) can be fitted to the admittance data to obtain the parameters. The parameters C_1 and C_0 calculated for unloaded crystal can be used as such during fitting under loaded condition as they are assumed to undergo no change.

The surface electrical impedance arising due to deposition of a rigid mass layer is given by[23]

$$\left|Z_m^L\right| = X_2 = 2\pi f L_2 = A\omega\rho_s \tag{8}$$

and the surface electrical impedance parameters for a crystal loaded with a Newtonian liquid are given by[23]

$$R_2 = X_2 = A\left(\frac{\omega\rho_{Liq}\eta_{Liq}}{2}\right)^{1/2} \tag{9}$$

The decay length or the penetration depth (boundary layer) of the shear wave in a liquid media, δ, defined as the length at which the amplitude reduces to 1/exp of the initial amplitude, is proportional to the fluid kinematic viscosity.[25]

Materials and Methods

Materials

Quartz crystals with a fundamental vibrating frequency of 5 and 10 MHz were obtained from International Crystal Manufacturing Co (Oklahoma City, OK). Glycerol USP was obtained from Fischer Scientific (Fair Lawn, NJ), PEG 400 and 8000 were obtained from Union Carbide Chemicals (Danbury, CT), ethylene glycol was obtained from Aldrich Chemical Co (Milwaukee, WI), sucrose was obtained from Pfizer (Groton, CT), and urea was obtained from United States Biochemicals (Cleveland, OH). All the chemicals used were of analytical grade. Deionized water equivalent to Milli-Q grade was used to prepare all solutions.

Crystal Characteristics and Surface Profile Analysis

Crystal blanks measured 0.538 inch in diameter. Electrodes were formed by vacuum evaporation of an adhesive layer of chromium of 10 nm thickness followed by a 100-nm thick layer of gold. Three types of crystals were used in the study. The first one with a fundamental vibrating frequency of 5 MHz had equal electrodes on both sides measuring 0.268 inch in diameter (Q1). The remaining 2 crystals with fundamental frequency of 5 and 10 MHz had different sized electrodes measuring 0.201 inch on one side and 0.391 inch on the other (Q2, 5 MHz and Q3, 10 MHz). Q1 crystals were used for initial standardization tests for correct frequency shift and resistance shift determination. Q2 and Q3 crystals were used for actual viscosity determination on liquid samples. The electrode finish was polished and not etched. Etched electrode surface can have surface features that are not small compared with the penetration depth of the acoustic waves in the fluid. For such a case, the effect of trapped fluid in the surface features can lead to deviation in the calculated values of R_2 and X_2 from the predicted values. To analyze surface roughness, NanoScope IV scanning probe microscope (Digital Instruments, Santa Barbara, CA) was used as an atomic force microscope in the contact mode. A standard silicon nitride tip with a nominal tip radius of 20 to 60 nm was used. The vertical resolution of the tip was less than 0.1 nm and lateral resolution was governed by the area of the crystal that was scanned for measurement. For a 5 μm × 5 μm area with 512 sampling points per line, the lateral resolution was 9.7 nm. A scan rate of 1.969 Hz was used for all measurements.

Impedance Measurement

The impedance analyzer used in the study was a Hewlett Packard HP4194A impedance/gain-phase analyzer (Agilent Technologies, Palo Alto, CA). The crystals were driven at 0.5 V with medium integration time and averaging of 1 second was used for all frequency scans in order to improve signal-to-noise ratio. Repeated scans were performed until stable values of total resistance and frequency shift were achieved. The impedance analyzer was interfaced with a personal computer through an Agilent 82357A GPIB interface card and data collection was achieved by using a data acquisition program written in National Instruments' programming language Labview. Crystals were mounted and bonded to a metal holder that was further connected to the terminals of the impedance analyzer through an assembly of 2 kelvin clips and 4 75-ohm BNC coaxial cables to enable a 4-terminal pair impedance measurement configuration. The entire assembly comprising the crystal and the metal casing, which was used to cover the crystal during measurements in order to avoid air interference effects, were enclosed in a temperature control water jacket and the temperature was maintained at 25°C ± 0.5°C. No o-ring or any kind of holder was directly placed or stuck on the crystal. Temperature was measured with the help of a thermocouple inserted into the liquid sample through a small leak proof opening in the water jacket. An airtight seal between the crystal assembly and the water jacket was achieved by using vacuum grease to prevent any effect of evaporation on density and viscosity. All the param-

eters for the unloaded crystal, ie, R_1, L_1, C_1, and C_0 were obtained by nonlinear fitting of the total admittance model (Equation 7) to the admittance frequency data. These parameters were used in subsequent experiments, under loaded conditions, to calculate resistance and reactance shifts.

Frequency and Resistance Shift Measurement

Different definitions of the frequency shift and resistance shift calculated for these characteristic frequencies under loaded conditions exist in the literature.[26] Some authors define frequency shift as that occurring in the position of Z_{min} (frequency at minimum impedance), ie, Δf_{Zmin},[27,28] which is the same as the shift in f_{Ymax}, whereas others consider the frequency shift as shift in frequencies at G_{max} (frequency at conductance maximum), ie, Δf_{Gmax} under unloaded and loaded conditions.[14,21,28,29] Kipling et al[30] define series resonant frequency as the frequency at which phase is 0, $\Delta f_{\theta=0}$. All these frequencies are the same under conditions of no load but begin to differ as load is added and as load properties change. To test this, glycerol-water mixtures of known density and viscosity were tested with Q1 crystals and characteristic frequency, and resistance shifts were calculated as outlined in the next paragraph.

An impedance analyzer can simultaneously measure 2 parameters as a function of frequency, for example a G-B vs frequency or a Z-θ vs frequency measurement can be made. From G-B vs frequency scans, X_2 was calculated using Δf_{Gmax} values and R_2 was calculated as $\Delta (1/G_{max})$. Z-θ vs frequency scans were used to make 2 separate measurements. First, X_2 was calculated from Δf_{Zmin} values and R_2 was calculated as ΔZ_{min}. Second, X_2 was also calculated from $\Delta f_{\theta=0}$ and R_2 from $\Delta Z_{\theta=0}$.

Viscosity Measurement

Viscosity measurements were performed on aqueous solutions of sucrose, urea, PEG 400, glucose, ethylene glycol, and PEG 8000 at 25°C using Q2 and Q3 crystals. Eight to 10 µL of the liquid was placed on the smaller electrode by forming a drop of the liquid on the electrode. Sufficient time was allowed for the drop to attain thermal equilibrium and reach the set temperature, which was being continuously monitored, before performing frequency scans. The thermocouple was removed once the set temperature was reached. Total resistance and frequency shifts were calculated from the G-B vs frequency scans. Calibration of the crystals was done with glycerol-water mixtures of known density[31] and viscosity[32] in order to experimentally determine the constant "A," in Equation 5, separately for each crystal. Each solution was analyzed 3 times and the results were averaged. Between each measurement, the crystal was thoroughly rinsed in deionized water followed by ethanol and dried in nitrogen until its initial values of resonant frequency and resistance under conditions of no load were obtained. If the initial value of frequency and resistance could not be obtained within 50 Hz and 5 ohms, respectively, of the new unused crystal, the crystal was not used any further and was discarded. Wiping off the crystal, in order to clean and dry it, was avoided as this can lead to electrode surface damage and make the surface rough. A rough surface can lead to fluid trapping and increased values of resistance and frequency shifts in a way similar to an etched electrode as explained earlier.[24]

Results and Discussion

Measurement of True Frequency and Resistance Shifts

Figure 3 shows the effect of increasing viscosity-density product, achieved by means of glycerol-water mixtures at 25°C, on the values of R_2 and X_2 for a Q1 crystal. The values of R_2 and X_2 were calculated from the resonance frequency shifts that occur between different characteristic frequencies. The frequency shifts were measured between frequencies of G_{max}, Z_{min}, and $\theta = 0$ for unloaded and loaded crystal. X_2 values were calculated from these frequency shifts. R_2 values were calculated from the difference between resistance at these frequencies under loaded and unloaded conditions. For Equation 9 to hold true for a Newtonian system (glycerol-water mixture) both R_2 and X_2 should vary linearly with $\sqrt{\rho\eta}$ and should be equal.

From Figure 3 it can be seen that at low values of $\sqrt{\rho\eta}$, R_2 and X_2 for all the frequency shifts are nearly equal but as increases further these values begin to diverge and move away from each other. The characteristic shifts in resistance (R_2) and reactance (X_2) for frequencies at Z_{min} and $\theta = 0$ tend to move away from linearity at high values of $\sqrt{\rho\eta}$. X_2 values calculated from shift in Δf_{Zmin} show a positive deviation, whereas those calculated from $\Delta f_{\theta = 0}$ show a negative deviation from linearity. On the contrary, R_2 values calculated as $\Delta Z_{\theta=0}$ show a positive deviation whereas those calculated from ΔZ_{min} show a slight negative deviation from linearity. Thus, these frequency and resistance shifts could not be used for viscosity analysis of fluids as they do not follow the expected linear trend for a Newtonian fluid. The reasons for such a nonlinear behavior were not investigated as they were beyond the scope of the present work.

However, the significant observation, from the point of view of the present study, is that the values of R_2 and X_2 calculated for shifts in peak conductance frequencies (Δf_{Gmax}) show a linear trend ($r^2 = 0.9997$ for R_2 and 0.9991 for X_2) and are nearly equal, which should be the case for a Newtonian liq-

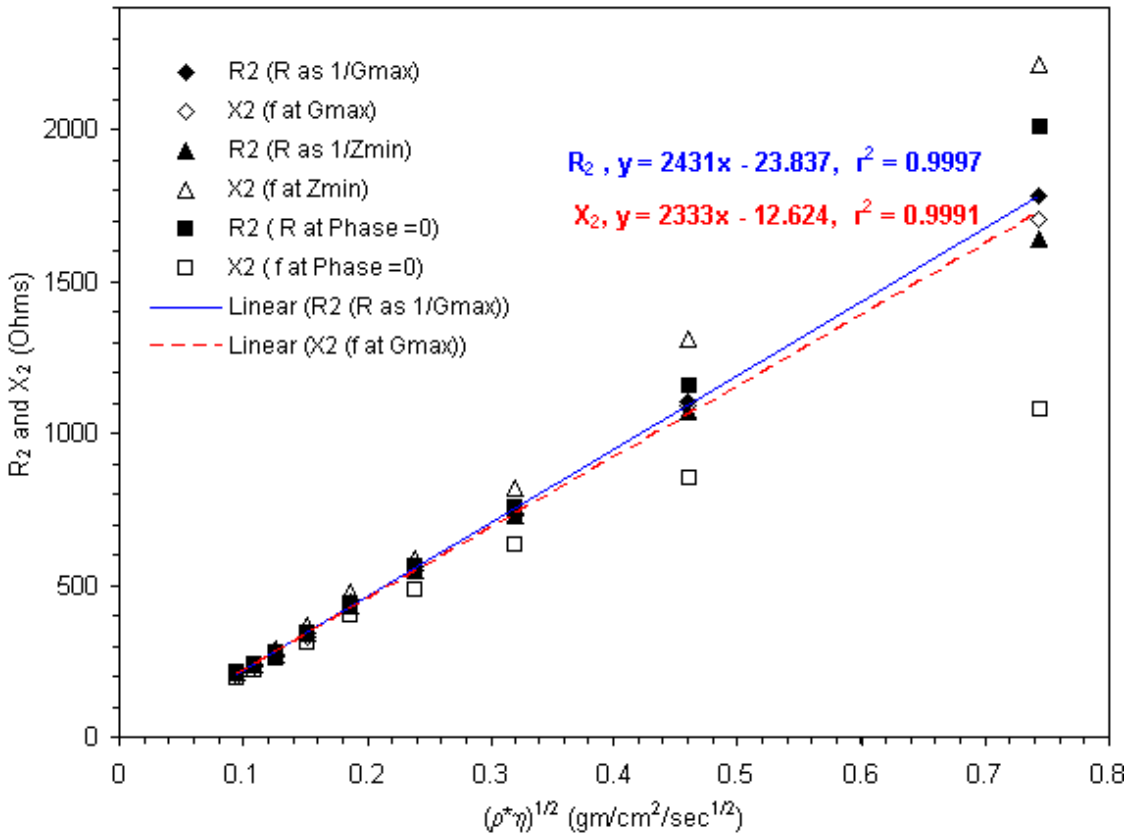

Figure 3. Effect of increasing density-viscosity product for glycerol-water mixtures at 25°C on X_2 values calculated for different frequency shifts and R_2 values for those frequencies for a Q1 crystal (5 MHz, 0.268"/0.268" electrodes). Solid symbols represent R_2 and open symbols indicate X_2 values. (◆,◇) Shift between peak conductance frequencies, (▲,△) shift between impedance minimum frequencies, (■,□) shift between frequencies at phase = 0.

uid. Thus, the true frequency shift for the study of fluid viscosity was defined as the difference between frequencies at peak conductance, and the true resistance shift was defined as difference between $1/G_{max}$ under loaded and unloaded conditions. For all the subsequent viscosity experiments, these shifts were noted and used for viscosity calculations.

A small difference that does exist between calculated R_2 and X_2 values for shift in Δf_{Gmax} needs to be explained. Whereas, R_2 is a direct function of inverse of G_{max}, X_2 is a calculated value, which directly depends on L_2 or indirectly on the frequency shift. As the accuracy of the frequency shift depends on the resolution of the frequency scan, so would the accuracy of X_2.

The HP4194A impedance analyzer can collect 401 points in the specified frequency scan range. On loading the crystal with the liquid, the conductance-frequency curve gets broader and flatter.[28] Thus, on liquid loading, the frequency scan range has to be increased in order to scan the crystal around the resonance frequency. This leads to a decrease in frequency resolution. However, this does not explain the fact that R_2 and X_2 deviate further from each other as the density-viscosity product increases, with R_2 increasing over X_2. The deviation in R_2 and X_2 is probably due to a small contribution from elastic storage in glycerol-water mixtures. Glycerol-water mixtures have been shown to exhibit some viscoelastic character at high megahertz frequencies at high glycerol concentration.[33] In Figure 3, a $\sqrt{\rho\eta}$ of 0.7435 g/cm^2/sec$^{1/2}$ corresponds to 80% glycerol wt/wt. This observation of viscoelasticity of a solution leading to differences in R_2 and X_2 values is dealt with later in the section where the results of rheological analysis of PEG 8000 are discussed.

Viscosity Measurement of Newtonian Fluids

During viscosity measurement experiments, due attention was given to the penetration depth of the acoustic waves in the fluid and the placement of the liquid on the electrode as this can have a significant bearing on the reproducibility of the results. The penetration depth (δ) of the acoustic shear wave in a liquid, which varies with the kinematic viscosity,[19] was greatest for 40% wt/wt sucrose solution at 530 nm for a 5-MHz crystal and 370 nm for a 10-MHz crystal. It was least for 10% wt/wt urea solution at 246 nm for a 5-MHz crystal and 174 nm for a 10-MHz crystal. For all the other liquids tested, the penetration depth was within this range as their kinematic viscosities were lower than that of 40% wt/wt sucrose solution and greater than that for 10% wt/wt urea solution. The liquid drop height was easily in excess of this height and was measured at around 1.5 to 2 mm.

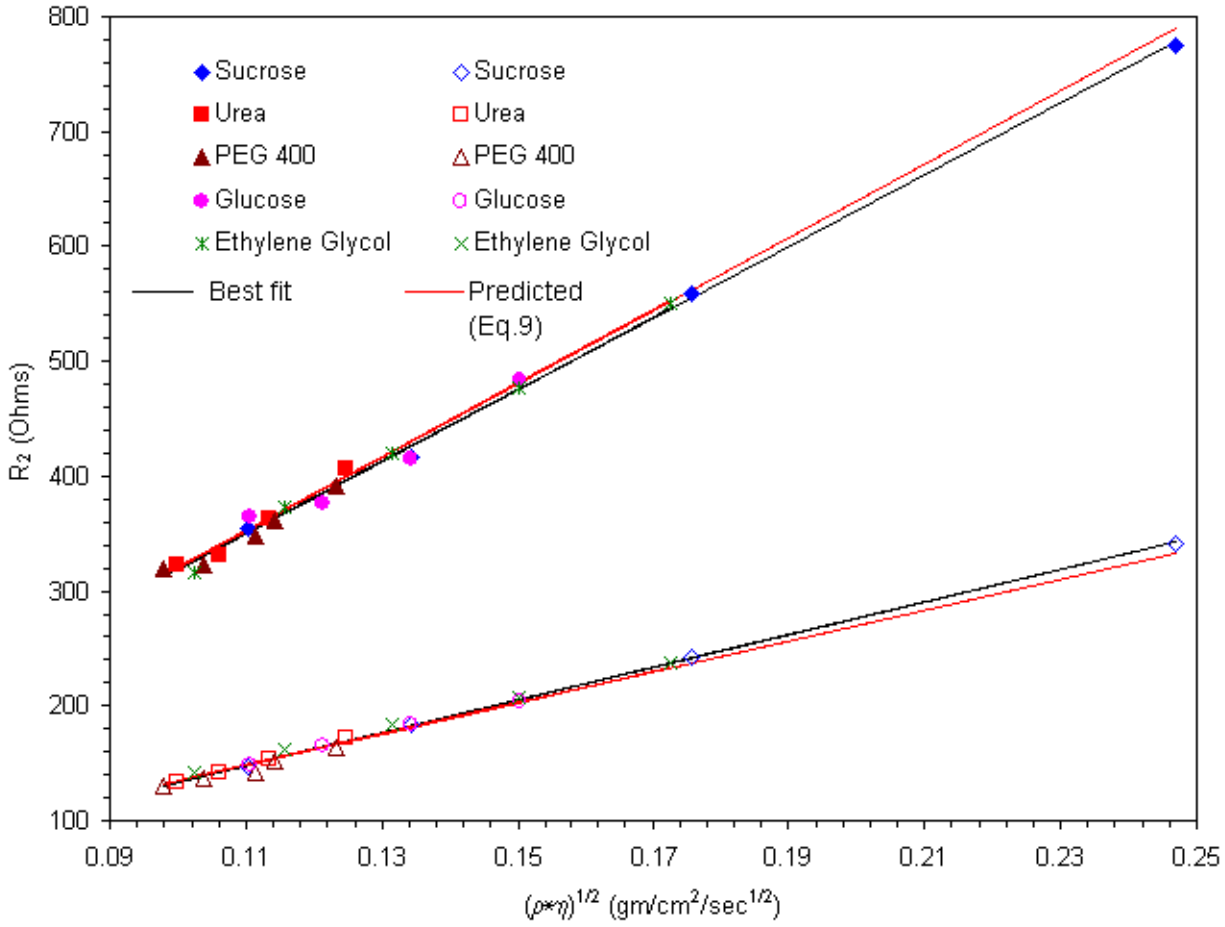

Figure 4. Effect of increasing density-viscosity product for different solutions on R_2 values at 25°C. Solid symbols represent results for Q2 crystal (5-MHz, 0.201-inch/0.391-inch electrodes) and open symbols represent the results for Q3 crystal (10-MHz, 0.201-inch/0.391-inch electrodes). The lines represent best fit to the data and the predicted response (Equation 9).

Enough volume of the liquid was added to ensure maximum coverage of the electrode without spilling the liquid on the electrode-free region of the crystal blank. This was critical for 3 reasons. First, any spillage of the liquid beyond the electrode leads to fringe effects. Fringe effects are observed when the electrode and electrode free regions of the crystal are simultaneously exposed to the liquid, which leads to poor reproducibility in the results as in such a case the total area exposed to the liquid is hard to control. This happens because in quartz crystals, a small region beyond the electrode regions also vibrates when a potential is applied and is thus piezoelectrically active. Second, such a placement of the liquid ensures equal area coverage by different liquids. This was significant as crystal response varies with the area covered. Third, the positioning of the drop on the electrode is also critical. The sensitivity of the quartz crystal to any external media varies with the positioning of the load. It is maximum at the center and then decreases in a Gaussian fashion radially outwards.[15] Thus, a small volume of liquid placed at the center will bring about a greater shift in the frequency and resistance than the same volume placed slightly off center. Complete coverage of the electrode ensured uniformity in drop placement as well.

Figure 4 and Figure 5 show the variation in R_2 and Δf respectively, with increasing $\sqrt{\rho\eta}$ for different solutions of small molecules for both Q2 and Q3 crystals. The figures also show the best fit lines to the data and the trends predicted by Equation 9 (R_2, Figure 4) and Equation 1 (Δf, Figure 5). It can be observed from the figures that both resistance and frequency shifts are linear with $\sqrt{\rho\eta}$ for both Q2 and Q3 crystals. A linear increase in resistance and frequency shifts for the liquids tested indicates a Newtonian behavior of these liquids. The data are also consistent with the predicted trends within the experimental error.

Table 1 shows the reported values of densities and viscosities[34,35] for liquids tested in this study at 25°C. The calculated values of viscosities for different liquids tested at 25°C have been tabulated in Table 2 for Q2 crystals and Table 3 for Q3 crystals. The reported values of fluid densities were used to calculate fluid viscosities. The significant observation from Table 2 and Table 3 is that the values of R_2 and X_2 were nearly equal for almost all the liquids tested, for both crystals, which again signifies that the liquids behaved as Newtonian

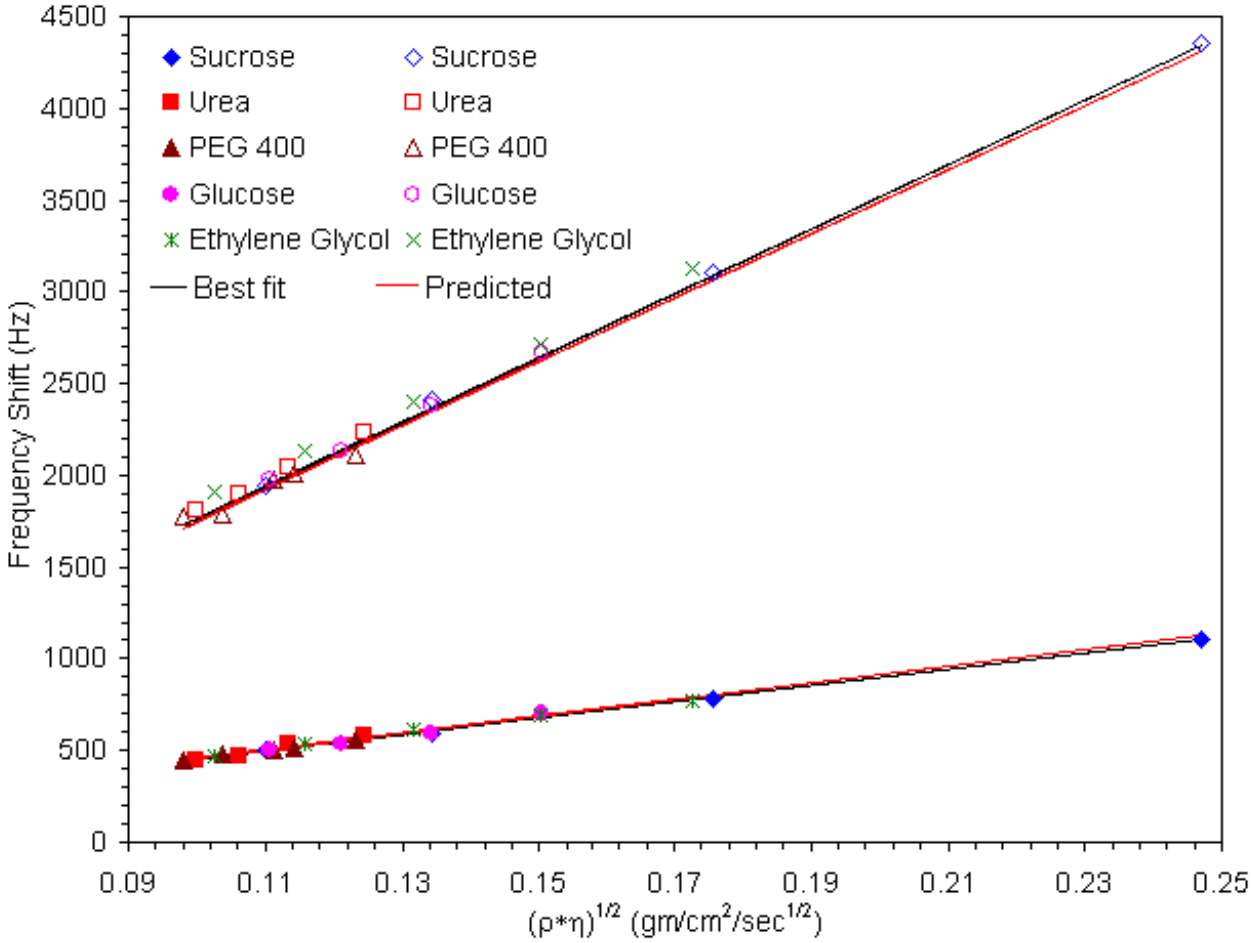

Figure 5. Effect of increasing density-viscosity product for different solutions on frequency shifts at 25°C. Solid symbols represent results for Q2 crystal (5-MHz, 0.201-inch/0.391-inch electrodes) and open symbols represent the results for Q3 crystal (10-MHz, 0.201-inch/0.391-inch electrodes). The lines represent best fit to the data and the predicted response (Equation 1).

fluids. Some differences that arise in the calculated values of R_2 and X_2 are probably due to the issue of frequency resolution and accuracy of X_2 calculation, ie, experimental error as discussed earlier. R_2 can exceed X_2 in the case of a contribution form elastic storage of energy for a viscoelastic fluid. However for liquids in Table 2 and Table 3, where R_2 does exceed X_2, the differences are probably not due to any viscoelastic contribution because these liquids have been shown to be purely viscous at the concentrations and frequencies tested.[34] Besides, even if there was some storage of energy occurring it would be insignificant as these differences are too small to amount to any significant viscoelasticity.

In certain cases, for example 10% to 40% wt/wt ethylene glycol solutions for Q2 crystals, X_2 exceeds R_2 (Table 2) and this could be interpreted as a contribution from mass deposition (Equation 8). However, this does not hold true for the same solutions studied for a 10-MHz Q3 crystal (Table 3). Had interference from mass deposition been the case, X_2 would have exceeded R_2 for both Q2 and Q3 crystals for the same solutions. For a Newtonian liquid, an increase in X_2 over R_2 can also occur if the crystal surface is not smooth and some liquid is trapped within these surface features.[19,24] The electrode surface can be considered smooth and the effect of fluid trapping negligible if the ratio of the surface feature height (h) to the penetration depth (δ) is much less than unity ($h/\delta << 1$).[19] The root mean square roughness (rms) calculated for Q2 and Q3 crystals, by atomic force microscopy, was ≈ 1 nm and < 1 nm respectively. The calculations based on the method of intercepts as given by Thiesen et al[19] resulted in feature heights of 1.5 nm and 0.6 nm for Q2 and Q3 crystals respectively. These measured and calculated heights were much less than the calculated penetration depths for various liquids for Q2 and Q3 crystals. All these observations point to the fact that inequality in R_2 and X_2 is just experimental and not due to any mass deposition or surface roughness effects.

While recording frequency scans, a cyclic variation (small decrease followed by an increase) in the values of G_{max} was noted. Reddy et al[27] have attributed such cyclic variation in resistance ($1/G_{max}$) to the interference from a small component of longitudinal/compressional waves that is present in an AT cut crystal due to certain flexure modes, besides the predominant shear waves that are due to the shear vibration mode. To consider this effect, repeated frequency scans were conducted and data were recorded when a maximum was

Table 1. Reported Values of Density and Viscosity at 25°C for Solutions Used in This Study

Solution	Solution Strength	Density (gm/cc) 25°C	Viscosity (cP) 25°C
Sucrose*† (% wt/wt)	10	1.038	1.17
	20	1.081	1.67
	30	1.125	2.75
	40	1.175	5.19
Urea* (% wt/wt)	10	1.024	0.97
	20	1.051	1.07
	30	1.080	1.19
	40	1.109	1.40
PEG 400* (mg/mL)	20	1.001	0.96
	40	1.038	1.04
	60	1.069	1.16
	80	1.081	1.21
	100	1.094	1.39
Glucose* (% wt/wt)	10	1.036	1.18
	15	1.057	1.39
	20	1.079	1.67
	25	1.105	2.05
Ethylene Glycol* (% wt/wt)	10	1.010	1.04
	20	1.023	1.31
	30	1.036	1.67
	40	1.049	2.15
	50	1.062	2.81

* Reported from Kurosawa et al.[34]

† Reported from James et al.[35]

noted in the cyclic change in G_{max} values. This method was kept uniform for all the solutions, and viscosity was calculated by using Equation 10. To take into account the effect of a small inequality in calculated values of R_2 and X_2, the following equation was used for calculation of viscosity as indicated by Mason et al and Barlow et al[5,36]:

$$\eta_{Liq} = \frac{2R_2X_2}{A^2\rho_{Liq}\omega} \qquad (10)$$

In case of R_2 and X_2 being equal, the equation reduces to the relationship given by Equation 9. The calculated viscosities, based on these parameters, were found to be reproducible and consistent with the viscosities reported in the literature (within experimental error). Besides, no significant difference was observed in the viscosities measured at 5 MHz and 10 MHz. This was expected as Newtonian fluids do not exhibit any change in measured viscosity with the frequency of measurement.

Before using this technique for mass and viscosity measurement one must be aware of the amount of load that can be safely placed on the crystal without affecting its accuracy. The loading has to be small such that the load impedance is not appreciable in comparison to the quartz impedance (small loading approximation).[15,28] In the case of too much loading there is a reduction in the sensitivity of the frequency shift to the areal mass-density or density-viscosity product of the liquid load and ultimately a saturation is achieved in the frequency shift.[28] In such a case the BVD model is no longer valid and an advanced form of the same, the transmission-line model (TLM), has to be applied, which is more rigorous but time-consuming as well. Cernosek et al[37] have calculated the tolerance limits of the load for the small loading approximation to be valid and for the application of the BVD model to a vibrating quartz crystal. For mass deposits, this limit is reached at a deposit density of 5 mg/cm^2. Stockbridge[38] suggested that the added mass should not be an appreciable fraction of the crystal mass and should be less than $1/10^5$ of it. For liquid loaded resonators, small load limit is reached at viscosity density product of ~1000 g^2/cm^4/sec. These limits produce load mechanical impedance to quartz mechanical impedance ratio (Z_s^L/Z_q) in excess of 0.1 (≈0.17 and ≈0.2, respectively). Many authors consider a ratio of 0.1 to be reliable for accurate determination of parameters using the BVD model.

Deviation from Newtonian Behavior

Table 4 shows the results for viscosity measurement experiments conducted on aqueous solutions of PEG 8000. Viscosities have been calculated using Equation 10 and reported values of densities. A large negative variation can be noted between the reported low shear rate viscosities[39] and calculated viscosities. This negative variation increases with an increase in the wt% of PEG 8000 and also with the frequency at which the measurements are conducted, ie, the measured viscosities were lower for 10-MHz crystal as compared with 5-MHz crystal.

Figure 6 shows the change in R_2 and X_2 values for PEG 8000 solutions and compares these with the trend for Newtonian sucrose solutions. With an increase in the density-viscosity product, the parameters for PEG 8000 show a curvature, whereas the parameters for sucrose solution follow a linear trend. There is a reduction in the parameter values from the expected values with X_2 showing a greater reduction than R_2. The extent of reduction increases with the increase in the measurement frequency. This trend is typical for viscoelastic fluids that exhibit a component of stored energy at high frequencies and whose complex viscosity comprises a loss and storage component. The modulii are frequency dependent and storage modulus shows an increase with the frequency of measurement. Thus, at higher frequency a greater deviation is observed from the linear Newtonian behavior.

For a pure Newtonian fluid, molecular reorientation or relaxation time (τ) is small enough even at high frequencies and the molecules are able to reorient themselves with the applied stress and all the applied energy is lost in the process

Table 2. Calculated Viscosities for Different Small Molecule Solutions at 25°C for Q2 Crystals. Frequency Shift (ΔF) and Resistance Increase (R_2) Have Also Been Tabulated Along With Calculated Values Of X_2. All Values are an Average of 3 Experiments

Solution	Solution Strength	Frequency Shift (Hz) (± SD, *n* = 3)	R_2 (Ohms) (± SD, *n* = 3)	X_2 (Ohms) (± SD, *n* = 3)	Calculated Viscosity (cp) (± SD, *n* = 3)	Variation* (%)
Sucrose (% wt/wt)	10	500, (11)	354, (7)	351, (8)	1.17, (0.05)	-0.05
	20	593, (6)	417, (2)	417, (5)	1.57, (0.02)	-6.14
	30	784, (12)	558, (5)	551, (8)	2.67, (0.06)	-2.89
	40	1103, (18)	776, (9)	776, (13)	5.00, (0.14)	-3.67
Urea (% wt/wt)	10	447, (6)	323, (3)	314, (4)	0.97, (0.02)	-0.63
	20	469, (2)	331, (1)	330, (1)	1.01, (0.004)	-5.21
	30	531, (2)	362, (4)	373, (3)	1.22, (0.01)	+2.52
	40	584, (4)	406, (2)	411, (3)	1.47, (0.02)	+4.83
PEG 400 (mg/mL)	20	447, (2)	319, (1)	314, (2)	0.97, (0.01)	+1.42
	40	475, (6)	323, (1)	333, (5)	1.01, (0.01)	-2.72
	60	500, (11)	348, (7)	351, (8)	1.11, (0.03)	-3.89
	80	516, (11)	361, (8)	362, (8)	1.18, (0.04)	-2.56
	100	556, (18)	392, (5)	390, (13)	1.36, (0.05)	-1.94
Glucose (% wt/wt)	10	505, (2)	365, (2)	355, (2)	1.22, (0.01)	+3.39
	15	540, (4)	377, (4)	380, (3)	1.32, (0.01)	-5.09
	20	591, (6)	416, (3)	415, (3)	1.56, (0.02)	-6.62
	25	703, (2)	483, (4)	493, (2)	2.10, (0.03)	+2.63
Ethylene Glycol (% wt/wt)	10	472, (8)	316, (5)	331, (6)	1.01, (0.03)	-2.72
	20	540, (17)	374, (5)	379, (11)	1.35, (0.06)	+3.11
	30	616, (4)	420, (4)	433, (2)	1.71, (0.02)	+2.39
	40	696, (11)	478, (4)	489, (7)	2.17, (0.05)	+0.94
	50	775, (18)	551, (6)	544, (14)	2.75, (0.10)	-1.97

* From reported data.

as the fluid deforms with the applied stress. For such a system, the product $\omega\tau$ is much less than unity. With an increase in molecular size, or concentration, of the solute the intermolecular interactions in the solution become intense and there is an increase in the "cohesiveness" of the system. This results in an increase in the relaxation time. As $\omega\tau$ approaches unity, relaxation time approaches $1/\omega$ and all the molecular motions are not able to relax or reorient in the timescale of a single oscillation. As a result, some energy begins to get stored in the system, and there is a decrease in the apparent viscosity of the system. Therefore, as $\omega\tau >> 1$ the fluid begins to get more viscoelastic and stores greater energy. The result of such a decrease in apparent viscosity is reflected in the decrease in R_2 and X_2 values as compared with Newtonian fluids in Figure 6. However, X_2 values are found to be even lower than the R_2 values. The reason for this is the decrease in the fluid penetration depth. As the apparent viscosity decreases, so does the fluid penetration depth, which is proportional to the kinematic viscosity of the vibrating load. This implies that the effective load of the fluid that entrains with the crystal is reduced, resulting in further reduction of the frequency shift or L_2 or X_2 values.

From Figure 6, 2 significant observations can be made. First, as the density-low shear rate viscosity product increases, there is an increasing deviation in both the calculated parameters, R_2 and X_2, for PEG 8000 from the linear trend that is followed by Newtonian fluids like aqueous sucrose solutions. This has already been explained. Second, as this is happening, the difference between R_2 and X_2 also goes on increasing. This difference between R_2 and X_2 has been calculated to be a measure of the energy stored in the system and is proportional to the frequency-dependent storage modulus (G') of the liquid. The product of R_2 and X_2 is proportional to the loss modulus (G″) of the liquid.[40]

$$G' = \frac{R_2^2 - X_2^2}{A^2 \rho_{Liq}} \tag{11}$$

$$G'' = \frac{2R_2 X_2}{A^2 \rho_{Liq}} \tag{12}$$

Thus, as the concentration of PEG 8000 is increased, a greater storage component and a larger deviation of the loss modulus from the loss modulus of a Newtonian liquid ($G''= \eta\omega$) will result. As frequency of measurement is increased, less time is allowed for the molecules to reorient. Therefore, a greater fraction of molecules is unable to relax or reorient and greater energy is stored in the system.

Figure 7 shows the variation in the storage and loss modulii of PEG 8000 aqueous solution with concentration and frequency of measurement. At both the frequencies used for measure-

Table 3. Calculated Viscosities for Different Small Molecule Solutions at 25°C for Q3 Crystals. Frequency Shift (ΔF) and Resistance Increase (R_2) Have Also Been Tabulated Along With Calculated Values of X_2. All Values are an Average of 3 Experiments.

Solution	Solution Strength	Frequency Shift (Hz) (± SD, *n* = 3)	R_2 (Ohms) (± SD, *n* = 3)	X_2 (Ohms) (± SD, *n* = 3)	Calculated Viscosity (cp) (± SD, *n* = 3)	Variation* (%)
Sucrose (% wt/wt)	10	1946, (18)	147, (1)	145, (1)	1.14, (0.01)	-2.73
	20	2407, (53)	183, (1)	180, (4)	1.69, (0.05)	+0.93
	30	3107, (49)	243, (2)	232, (4)	2.77, (0.04)	+0.97
	40	4355, (55)	341, (2)	325, (4)	5.22, (0.10)	+0.67
Urea (% wt/wt)	10	1811, (5)	133, (1)	135, (0)	0.97, (0.00)	-0.39
	20	1894, (10)	141, (2)	141, (1)	1.05, (0.01)	-1.79
	30	2038, (21)	154, (3)	152, (1)	1.20, (0.03)	+1.13
	40	2229, (28)	172, (2)	166, (2)	1.43, (0.02)	+2.07
PEG 400 (mg/mL)	20	1775, (14)	130, (0)	132, (1)	0.95, (0.01)	-1.48
	40	1788, (3)	136, (0)	133, (0)	0.96, (0.00)	-7.23
	60	1975, (15)	142, (1)	147, (1)	1.08, (0.02)	-6.85
	80	2009, (14)	152, (2)	149, (1)	1.17, (0.02)	-3.60
	100	2110, (13)	163, (1)	157, (1)	1.29, (0.01)	-6.90
Glucose (% wt/wt)	10	1972, (28)	148, (2)	147, (2)	1.17, (0.03)	-1.08
	15	2128, (7)	165, (1)	158, (1)	1.36, (0.01)	-1.88
	20	2383, (19)	183, (2)	178, (2)	1.67, (0.01)	+0.10
	25	2664, (11)	204, (0)	198, (1)	2.03, (0.01)	-1.02
Ethylene Glycol (% wt/wt)	10	1906, (16)	141, (0)	142, (1)	1.10, (0.01)	+5.61
	20	2133, (15)	162, (0)	159, (1)	1.39, (0.01)	+6.20
	30	2397, (10)	183, (0)	178, (1)	1.74, (0.01)	+4.26
	40	2716, (16)	207, (1)	202, (1)	2.20, (0.03)	+2.44
	50	3125, (17)	238, (1)	232, (1)	2.88, (0.03)	+2.41

* From reported data.

Table 4. Reported and Calculated Viscosities for PEG 8000 at 25°C for Q2 and Q3 Crystals

Solution	Solution Strength	Density (gm/cc) 25°C	Reported Viscosity* (cP) 25°C	Calculated Viscosity (cP) (± SD, *n* = 3)		% Variation†	
				Q2	Q3	Q2	Q3
PEG 8000 (% wt/wt)	10	1.015	8.90	3.49, (0.29)	2.48, (0.12)	-60.79	-72.16
	20	1.032	20.20	6.04, (0.23)	4.65, (0.14)	-70.08	-76.99
	30	1.049	50.90	9.74, (0.24)	7.94, (0.08)	-80.87	-84.40
	40	1.067	126.50	17.02, (0.29)	13.42, (0.16)	-86.54	-89.39

* Reported Gonzalez-Tello et al.[39]

† From reported data.

ment, the loss modulus is greater than the storage modulus. This is not surprising as viscoelastic solutions behave this way as long as they are in the liquid regime. As the liquid begins to set into a gel, there is an increase in the cross-link formation in the system and the storage modulus begins to exceed the loss modulus. In addition, the storage modulus is higher at 10 MHz as compared with 5 MHz because of greater storage at higher frequency as has been explained.

Such deviations from a Newtonian behavior, as illustrated by Figures 6 and 7, not only emphasize the dynamic nature of fluids at high frequencies but also lends support to the necessity of measuring resistance shifts in addition to frequency shifts, instead of only the latter, while analyzing liquids for their rheological behavior. Together, both these shifts enable us to distinguish between pure viscosity and viscoelastic effects in addition to simple mass effects.

These results indicate that quartz crystal impedance analysis for nondestructive rheological testing of fluids is a promising technique for assessing viscosity of Newtonian fluids at low microliter volumes. Consistent and reproducible viscosity analysis of aqueous Newtonian fluids can be conducted by ensuring adherence to certain experimental safeguards. These precautions need to be strictly followed due to high sensitivity of the quartz crystals to changes in the material load, electrode surface morphology effects, and interference from compressional vibration mode. Besides Newtonian fluids, this technique has also been used for rheological characterization of non-Newtonian viscoelastic fluids although not

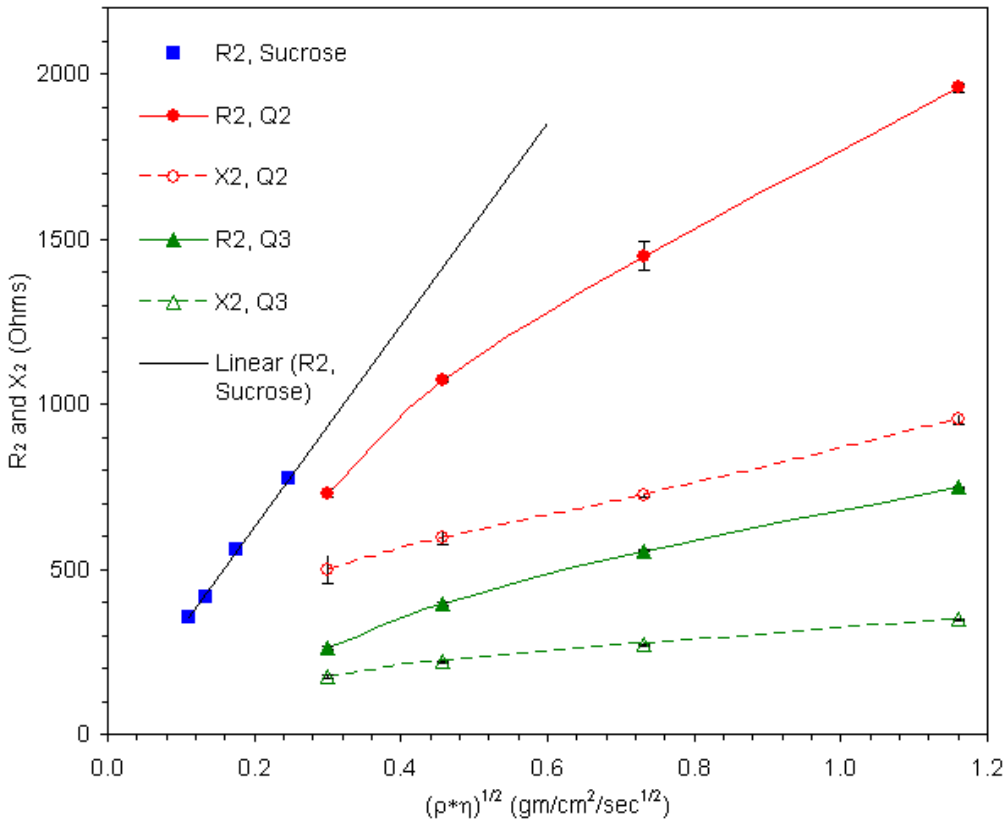

Figure 6. Calculated R_2 and X_2 values for a Newtonian fluid, aqueous sucrose solution, and a non-Newtonian fluid, aqueous PEG 8000 solution, as a function of increasing density-viscosity product at 25°C for Q2 (5-MHz, 0.201-inch/0.391-inch electrodes) and Q3 crystals (10-MHz, 0.201-inch/0.391-inch electrodes).

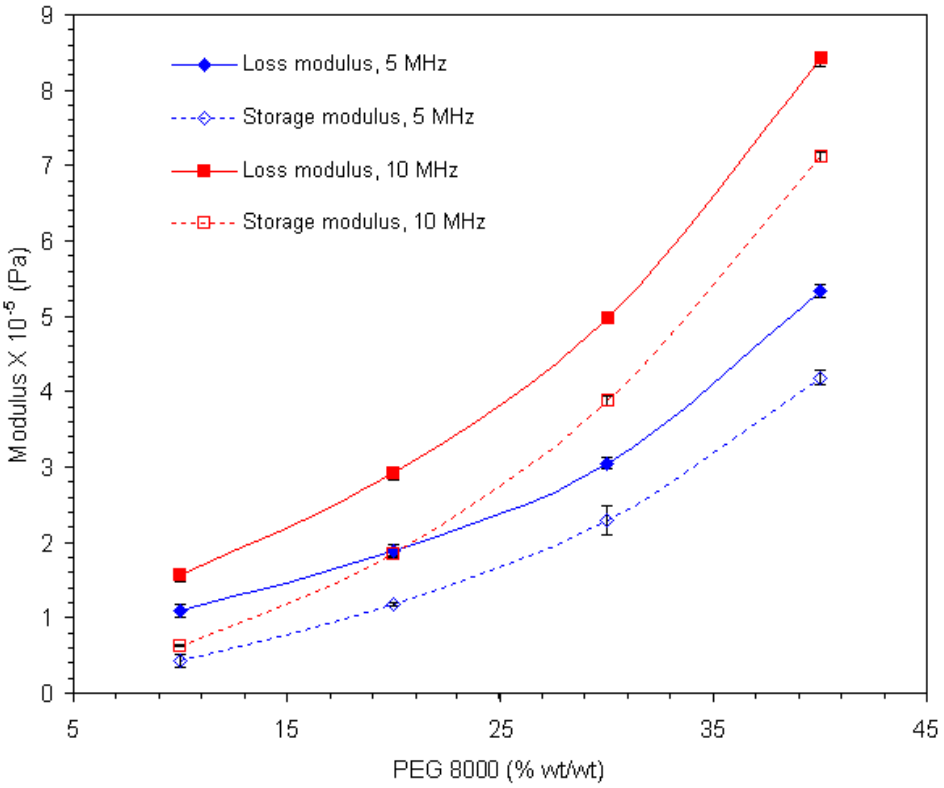

Figure 7. Storage and loss modulii for aqueous PEG 8000 solutions with increasing concentration for Q2 (5-MHz, 0.201-inch/0.391-inch electrodes) and Q3 crystals (10-MHz, 0.201-inch/0.391-inch electrodes). Solid symbols represent loss modulus and open symbols represent storage modulus.

at such low volumes. We envisage further studies on viscoelastic as well as oil-based liquid solutions and suspensions to realize the true potential for the application of quartz impedance analysis in non-Newtonian fluid rheology analysis at low microliter volumes.

CONCLUSION

Quartz crystal impedance analysis can provide reliable assessment of fluid rheological properties at low microliter volumes by simultaneous measurement of frequency and resistance shifts. Measured values of viscosity for solutions of sucrose, urea, PEG 400, glucose, and ethylene glycol, at frequencies of 5 and 10 MHz, were found to be consistent with the values reported in the literature, whereas for PEG 8000 measured viscosity values were found to be less than the low shear rate viscosities reported in the literature. This deviation from the reported values arises due to the frequency dependence of the energy stored and lost during each cycle for a viscoelastic fluid.

ACKNOWLEDGEMENTS

The authors would like to acknowledge financial supports from the National Science Foundation Industry/University Cooperative Research Center for Pharmaceutical Processing (http://www.ipph.purdue.edu/~nsf/aboutCPPR.html) and the University of Connecticut, Storrs, CT. The authors also thank Professor James F. Rusling for providing the scanning probe microscope for surface analysis and Jing Yang for her assistance with the technique.

REFERENCES

1. Macosko CW. Rheology: Principles, Measurement and Applications. New York, NY: Wiley-VCH; 1994.

2. Larson RG. The Structure and Rheology of Complex Fluids. New York, NY: Oxford University Press; 1999.

3. Kudryashov ED, Hunt NT, Arikainen EO, Buckin VA. Monitoring of acidified milk gel formation by ultrasonic shear wave measurements. High-frequency viscoelastic moduli of milk and acidified milk gel. *J Dairy Sci*. 2001;84:375-388.

4. Mason WP. Measurement of the viscosity and shear elasticity of liquids by means of a torsionally vibrating crystal. *Trans Am Soc Mech Eng*. 1947;68:359-370.

5. Mason WP, Baker WO, McSkimin HJ, Heiss JH. Measurement of shear elasticity and viscosity of liquids at ultrasonic frequencies. *Phys Rev*. 1949;75:936-946.

6. Hoummady M, Bastien F. Acoustic wave viscometer. *Rev Sci Instrum*. 1991;62:1999-2003.

7. Bruckenstein S, Shay M. Experimental aspects of use of the quartz crystal microbalance in solution. *Electrochim Acta*. 1985;30:1295-1300.

8. Kanazawa KK, Gordon JG II. The oscillation frequency of a quartz resonator in contact with liquid. *Anal Chim Acta*. 1985;175:99-105.

9. Kauzlarich JJ, Ross RA, Abdallah DS. A new electronic viscometer based on Rayleigh wave mechanics. *Tribotest*. 1998;5:135-143.

10. Buckin V, Kudryashov E. Ultrasonic shear wave rheology of weak particle gels. *Adv Colloid Interface Sci*. 2001;89-90:401-422.

11. Morray B, Li S, Hossenlopp J, Cernosek R, Josse F. PMMA polymer film characterization using thickness-shear mode (TSM) quartz resonator. P. IEEE Internat. Freq. Control Symp. PDA Exhibit. New Orleans, LA: Institute of Electrical and Electronics Engineers, New York, NY; 2002:294-300.

12. Calvo EJ, Etchenique R, Bartlett PN, Singhal K, Santamaria C. Quartz crystal impedance studies at 10 MHz of viscoelastic liquids and films. *Faraday Discuss*. 1997;107:141-157.

13. Bandey HL, Hillman AR, Brown MJ, Martin SJ. Viscoelastic characterization of electroactive polymer films at the electrode/solution interface. *Faraday Discuss*. 1997;107:105-121.

14. Ash DC, Joyce MJ, Barnes C, Booth CJ, Jefferies AC. Viscosity measurement of industrial oils using the droplet quartz crystal microbalance. *Meas Sci Technol*. 2003;14:1955-1962.

15. Buttry DA, Ward MD. Measurement of interfacial processes at electrode surfaces with the electrochemical quartz crystal microbalance. *Chem Rev*. 1992;92:1355-1379.

16. Martin SJ, Bandey HL, Cernosek RW, Hillman AR, Brown MJ. Equivalent-circuit model for the thickness-shear mode resonator with a viscoelastic film near film resonance. *Anal Chem*. 2000;72:141-149.

17. Sauerbrey G. The use of quartz oscillators for weighing thin layers and for microweighing. *Z Phys*. 1959;155:206-222.

18. Ferrante F, Kipling AL, Thompson M. Molecular slip at the solid-liquid interface of an acoustic-wave sensor. *J Appl Physiol*. 1994;76:3448-3462.

19. Thiesen LA, Martin SJ, Hillman AR. A model for the quartz crystal microbalance crystal response to wetting characteristics of corrugated surfaces. *Anal Chem*. 2004;76:796-804.

20. Nwankwo E, Durning CJ. Impedance analysis of thickness-shear mode quartz crystal resonators in contact with linear viscoelastic media. *Rev Sci Instrum*. 1998;69:2375-2384.

21. Reed CE, Kanazawa KK, Kaufman JH. Physical description of a viscoelastically loaded AT-cut quartz resonator. *J Appl Physiol*. 1990;68:1993-2001.

22. Lucklum R, Hauptmann P. Determination of polymer shear modulus with quartz crystal resonators. *Faraday Discuss*. 1997;107:123-140.

23. Bandey HL, Martin SJ, Cernosek RW, Hillman AR. Modeling the responses of thickness-shear mode resonators under various loading conditions. *Anal Chem*. 1999;71:2205-2214.

24. Martin SJ, Frye GC, Ricco AJ, Senturia SD. Effect of surface roughness on the response of thickness-shear mode resonators in liquids. *Anal Chem*. 1993;65:2910-2922.

25. Behrends R, Kaatze U. A high frequency shear wave impedance spectrometer for low viscosity liquids. *Meas Sci Technol*. 2001;12:519-524.

26. Arnau A, Jimenez Y, Sogorb T. Thickness-shear mode quartz crystal resonators in viscoelastic fluid media. *J Appl Physiol*. 2000;88:4498-4506.

27. Reddy SM, Jones JP, John Lewis T. Use of combined shear and pressure acoustic waves to study interfacial and bulk viscoelastic effects in aqueous polymeric gels and the influence of electrode potentials. *Faraday Discuss*. 1997;107:177-196.

28. Martin SJ, Granstaff VE, Frye GC. Characterization of a quartz crystal microbalance with simultaneous mass and liquid loading. *Anal Chem*. 1991;63:2272-2281.

29. Muramatsu H, Tamiya E, Karube I. Computation of equivalent circuit parameters of quartz crystals in contact with liquids and study of liquid properties. *Anal Chem*. 1988;60:2142-2146.

30. Kipling AL, Thompson M. Network analysis method applied to liquid-phase acoustic wave sensors. *Anal Chem*. 1990;62:1514-1519.

31. National Reserach Council. International Critical Tables of Numerical Data, Physics, Chemistry and Technology. New York, NY: McGraw Hill Book Company; 1926-1930.

32. Sheely ML. Glycerol viscosity tables. *Ind Eng Chem*. 1932;24:1060-1064.

33. Bund A, Schwitzgebel G. Viscoelastic properties of low-viscosity liquids studied with thickness-shear mode resonators. *Anal Chem*. 1998;70:2584-2588.

34. Kurosawa S, Tawara E, Kamo N, Kobatake Y. Oscillating frequency of piezoelectric quartz crystal in solutions. *Anal Chim Acta*. 1990;230:41-49.

35. James CJ, Mulcahy DE, Steel BJ. Viscometer calibration standards: viscosities of water between 0 and 60.degree.C and of selected aqueous sucrose solutions at 25.degree.C from measurements with a flared capillary viscometer. *J Phys D Appl Physiol*. 1984;17:225-230.

36. Barlow AJ, Lamb J. The visco-elastic behaviour of lubricating oils under cyclic shearing stress. *P Roy Soc Lond A Mat*. 1959;253:52-69.

37. Cernosek RW, Martin SJ, Hillman AR, Bandey HL. Comparison of lumped-element and transmission-line model for thickness-shear-mode quartz resonator sensors. *IEEE Trans Ultrason Ferroelectr Freq Control*. 1998;45:1399-1407.

38. Stockbridge CD. Resonance frequency versus mass added to quartz crystals. In: Behrndt KH, ed. Vacuum Microbalance Techniques. New York, NY: Plenum; 1966:193-205.

39. Gonzalez-Tello P, Camacho F, Blazquez G. Density and viscosity of concentrated aqueous solutions of polyethylene glycol. *J Chem Eng Data*. 1994;39:611-614.

40. Barlow AJ, Subramanian S. Experimental technique for the determination of the visco-elastic properties of liquids in the frequency range 5-75 Mc. *Brit J Appl Phys*. 1966;17:1201-1214.